

## Original article

# Local treatment of osteoporosis with alendronate-loaded calcium phosphate cement

Zhao Jindong, Tang Hai, Wang Jiayang and Li Gang

**Keywords:** local treatment of osteoporosis; alendronate-loaded calcium phosphate cement; trabecular bone microarchitecture; biomechanical properties; micro-CT drug delivery system

**Background** A new treatment strategy is to target specific areas of the skeletal system that are prone to clinically significant osteoporotic fractures. We term this strategy as the “local treatment of osteoporosis”. The study was performed to investigate the effect of alendronate-loaded calcium phosphate cement (CPC) as a novel drug delivery system for local treatment of osteoporosis.

**Methods** An *in vitro* study was performed using CPC fabricated with different concentrations of alendronate (ALE, 0, 2, 5, 10 weight percent (wt%)). The microstructure, setting time, infrared spectrum, biomechanics, drug release, and biocompatibility of the composite were measured in order to detect changes when mixing CPC with ALE. An *in vivo* study was also performed using 30 Sprague-Dawley rats randomly divided into six groups: normal, Sham (ovariectomized (OVX) + Sham), CPC with 2% ALE, 5%ALE, and 10% ALE groups. At 4 months after the implantation of the composite, animals were sacrificed and the caudal vertebrae (levels 4-7) were harvested for micro-CT examination and biomechanical testing.

**Results** The setting time and strength of CPC was significantly faster and greater than the other groups. The ALE release was sustained over 21 days, and the composite showed good biocompatibility. In micro-CT analysis, compared with the Sham group, there was a significant increase with regard to volumetric bone mineral density (BMD) and trabecular number (Tb.N) in the treated groups ( $P < 0.05$ ). Trabecular spacing (Tb.Sp) showed a significant increase in the Sham group compared to other groups ( $P < 0.01$ ). However, trabecular thickness (Tb.Th) showed no significant difference among the groups. In biomechanical testing, the maximum compression strength and stiffness of trabecular bone in the Sham group were lower than those in the experimental groups.

**Conclusions** The ALE-loaded CPC displayed satisfactory properties *in vitro*, which can reverse the OVX rat vertebral trabecular bone microarchitecture and biomechanical properties *in vivo*.

Chin Med J 2014;127 (22): 3906-3914

Osteoporosis is a skeletal disorder characterized by low bone mass and deterioration of bone microarchitecture resulting in bone fragility. As the aging population increases, the rising prevalence of osteoporosis-related injuries will have a dramatic impact on health care. Altered bone microarchitecture and diminished bone mineral density (BMD) ultimately lead to greater bone fragility and increased susceptibility to pathologic fracture.<sup>1</sup> The management of osteoporosis is among the greatest challenges faced by modern medicine. Indeed, the aging of the population is increasing the prevalence of osteoporosis, which is associated with tremendous psychological, social and economic burdens.<sup>2</sup> In China alone, there are approximately 13 million osteoporotic vertebral fractures annually.<sup>3</sup> At present, the mainstay of treatment relies on systemic medications intending to increase BMD, improve bone mass and bone microarchitecture, and most importantly, decrease fracture incidence.<sup>4,5</sup> However, the enormity of this problem will continue to result in a large population of patients who remain at significant risk for osteoporotic fracture despite medical optimization. New treatment targets should be identified via improvements in the knowledge of bone pathophysiology, bone remodeling, bone cells, intracellular signaling pathways and drug delivery. These improvements constitute evidence of the

considerable research efforts that are being expended to ameliorate osteoporosis.

A new treatment strategy is to target specific areas of the skeletal system that are prone to clinically significant osteoporotic fractures. We term this strategy as the “local treatment of osteoporosis”. This is topical application of anti-resorptive, bone formation agents or biological materials to treat osteoporosis, which can enhance the volumetric BMD, bone microstructure, and biomechanics of the local osteoporotic bone. Otsuka et al<sup>6</sup> injected calcium

DOI: 10.3760/cma.j.issn.0366-6999.20141670

Department of Orthopedics, the Fifth Hospital of Harbin City, Harbin, Heilongjiang 150040, China (Zhao JD)

Department of Orthopedics, Beijing Friendship Hospital, Capital Medical University, Beijing 100050, China (Tang H)

Department of Cardiac Surgery, Beijing An Zhen Hospital, Capital Medical University, Beijing 100029, China (Wang JY)

The Department of Orthopedics & Traumatology, Faculty of Medicine, CUHK-WHO Collaborating Centre for Sports Medicine and Health Promotion, The Chinese University of Hong Kong, Clinical Sciences Building, Prince of Wales Hospital, Shatin, Hong Kong, China (Li G)

Correspondence to: Prof. Tang Hai, Department of Orthopedics, Beijing Friendship Hospital, Capital Medical University, Beijing 100050, China (Email: tanghai@medmail.com.cn)

phosphate ceramics suspensions containing magnesium, zinc and fluoride into the right femur of ovariectomized (OVX) rats. The BMD and bone mechanical strength of the right femur were significantly higher than the left femur on day 28. Peter et al<sup>7</sup> used local delivery of zoledronate from coated orthopedic implants in osteoporotic rats. Twenty-five 6-month-old female Wistar rats were OVX for 6 weeks before the implantation to induce osteoporosis. The animals were randomly separated in five groups representing different zoledronate concentrations in the hydroxyapatite (HA), coating: 0, 0.2, 2.1, 8.5, and 16  $\mu\text{g}/\text{implant}$ . A remarkable result showed a window of zoledronate content (0.2 to 8.5  $\mu\text{g}/\text{implant}$ ) in which the mechanical fixation of the implant increased. Furthermore, Phillips et al<sup>8</sup> analyzed the effects of osteogenic protein-1 (OP-1; BMP-7) treatment on osteopenic ovine vertebral architecture and biomechanics. After creating an 8 mm diameter defect in the mid-vertebral body, sheep underwent intravertebral body implantation at two nonadjacent levels. Animals were euthanized 6 months after implantation. Histology showed varied degrees of bony healing in the injection sites. Histomorphometrically, OP-1 treated vertebrae showed improvements in percent bone of up to 38% and star volume of up to 55% compared to the control group. Improvements in whole vertebral body BMD were not detected for any treatment. But the above studies had some deficiencies, one was that the BMD of local osteoporotic bone had not always changed significantly; another was that local treatment effects would gradually disappeared when the local material release stopped.

Previous studies have shown the promising potency of the bisphosphonates (BPs) in reducing osteoporotic fracture due to their high affinity for bone mineral and powerful inhibitory effects on osteoclast-mediated bone resorption through suppressing osteoclast function, inhibiting osteoclast differentiation, and promoting osteoclast apoptosis.<sup>9-12</sup> Among the BPs, the most important is alendronate (ALE), which has already been widely used in the clinical treatment of systemic metabolic bone diseases.<sup>13</sup> However, BPs have undesirable effects such as gastrointestinal ulceration<sup>14,15</sup> and jaw osteonecrosis,<sup>16,17</sup> and also have low oral bioavailability, between 1% and 3% of the dose ingested.<sup>18</sup> On this basis, the development of a strategy for local administration of BPs becomes even more intriguing.

Calcium phosphate cement (CPC) is a most important biomaterial for medical application because of its excellent properties such as bioactivity, self-setting, injectability, and plasticity. The multi-porous structure makes it a natural lattice for bone tissue in growth when implanted in the body.<sup>19</sup> Different studies with CPCs have shown that they are highly biocompatible and osteoconductive materials, which can stimulate tissue regeneration.<sup>20-23</sup> As a drug delivery system (DDS), a clinical study indicated that CPC has distinct effects in curing and preventing osteoporosis.<sup>24</sup>

Although these studies reported the positive effects of

BPs and CPC osseointegration in osteoporosis, there is no experimental study that describes the effects of locally applied BPs combined with CPC in an osteoporotic animal or patient. Recently a new DDS using CPC containing three different ALE concentrations were developed:  $\beta$ -tricalcium phosphate ( $\beta$ -TCP), tetracalcium phosphate (TECP), HA, and dicalcium phosphate anhydrate (DCPA).<sup>25</sup> We hypothesized that the composite would display satisfactory properties *in vitro* when it is administered locally; the composite can improve trabecular bone microarchitecture and bone biomechanics in locally osteoporotic bone. Based on this, our study was designed to observe the effects of the composite in OVX rat spine as assessed by high-resolution micro-CT and biomechanical testing.

## METHODS

### *In vitro* study

#### *Specimen preparation and grouping*

The powdered CPC (ReboneGutai, Shanghai Rebone Biomaterials Co., Ltd, China) was mixed uniformly with ALE in four different concentrations (0, 20, 50 and 100 mg/g). From the paste, a series of 15 standard cylinders, 6 mm in diameter and 12 mm in length, of each composite was formed in metal molds without any compression (liquid/solid: 0.5). After a hardening period of 4 hours, they were maintained for 24 hours at 37°C and 100% relative humidity in a thermostatically incubator. The specimens were stored in a desiccator for further use. The specimens were divided into four groups ( $n=5$  for each group): CPC (control group), 2% ALE group (CPC containing 2% ALE), 5% ALE group (CPC containing 5% ALE), and 10% ALE group (CPC containing 10% ALE).

#### *Characterization of the specimens*

The chemical structure of the specimen was characterized by Fourier transform infrared spectroscopy (FTIR, Nicolet 750, Nicolet Co., USA) in transmission mode. The morphology and microstructure of the specimens were observed using scanning electron microscope (SEM, H-800, Hitachi Co., Japan). Before performing SEM, the specimens were dried and coated with gold.

#### *Measurement of setting time*

The specimens were tested to the reference ASTM C191-03 standard,<sup>26</sup> using a Vicat apparatus (Shanghai Luda Experimental Instrument Co., Ltd. Shanghai, China), which had a movable rod of (300.0 $\pm$ 0.5) g mass and a removable needle of (1.0 $\pm$ 0.05) mm diameter fixed at the end of the rod. The Vicat needle was carefully lowered vertically on the surface of the newly shaped specimens and kept there for 5 seconds. The indentation was repeated at intervals of 30 seconds until the specimen hardened. The initial setting time was calculated as when the needle did not penetrate more than 2 mm into the specimen; the final setting time was also calculated when no mark was visible after the needle was applied to the surface.<sup>27</sup>

#### *Release testing*

The released quantity of ALE was measured as follows.

Specimens were introduced into 3 ml of phosphate buffer (pH 7.25) in a 15 ml test tube with a cap. The tube was fixed on the specimen holder in a thermostatically regulated water bath maintained at  $(37.0 \pm 0.1) ^\circ\text{C}$ , and shaken at 90 r/min. During the release test, the entire dissolution medium was replaced with fresh buffer at 24 hours. Supernatant (1.0 ml) of the specimen media was collected and rinsed in an iron (III) chloride/perchloric acid solution so that the suspended ALE could be completely extracted into the aqueous phase as a previous study described.<sup>28</sup> The ALE concentration in the iron (III) chloride/perchloric acid extraction was examined using ultraviolet (UV) spectrophotometry. The analytical methods were validated according to linearity, precision, accuracy, and specificity.<sup>28</sup> To determine the duration of likely biological activity, the release of ALE was observed over a period of 21 days.

#### *Mechanical testing*

The compressive strength of CPC specimens mixed with several concentrations of ALE was investigated to detect changes in the mechanical properties. The specimens were produced in the same way as in the release study and the same concentrations of ALE were used. Comparison cylinders of CPC without ALE were tested as controls. For each group, five standard-sized cylinders were produced. All cylinders were tested on an Instron machine (Instron 5 848 MicroTester, Instron, Co., USA) under axial compression at a speed of 0.1 mm/second. Each testing was performed five times and the average value was calculated.

#### *Cell-culture and cytotoxicity assay*

Rat mesenchymal stem cells (MSCs) were propagated at a density of  $1 \times 10^5/\text{cm}^2$  in T-25 flasks (Corning, USA) with basal culture media containing alpha Modified Eagle Medium, 15% fetal bovine serum (FBS), 2 mmol/L L-glutamine, 100 IU penicillin, 100  $\mu\text{g}/\text{ml}$  streptomycin, and 2.5  $\mu\text{g}/\text{ml}$  fungizone (Life Technologies, UK). The cells grew for three days, then the medium was replaced with fresh medium, and adherent cells grew to 80% confluence to obtain samples herein defined as passage zero (P0) cells. Cells were then detached from the T-25 flasks by 0.25% trypsinization, FBS terminated digestion, PBS washed. Cell number and viability were checked using the trypan blue dye exclusion test.

The 5th passage (P5) cells were plated at a density of  $1 \times 10^4/\text{ml}$  per well in 96-well plates containing sterile 0.2 ml eluant (the substance referred to as eluant is the same as the samples produced during the analysis of the release kinetics and the eluant was collected at 24 hours) of CPC alone (control), and CPC with 2% ALE, 5% ALE, and 10% ALE. Plates were cultured using standard conditions, in a humidified atmosphere at  $37^\circ\text{C}$  with 5%  $\text{CO}_2$  for up to 7 days. Cytotoxicity was evaluated with the 3-(4,5-dimethylthiazol-2-yl)-2,5-diphenyltetrazolium bromide (MTT, Roche Diagnostics, Germany) assay following a standard protocol.<sup>29</sup>

#### *In vivo study*

##### *Animals experimentation*

Thirty female Sprague-Dawley rats weighing  $(230 \pm 20)$  g

were housed individually in cages. All received regular rodent feed and were raised in an air-conditioned environment with a relative steady temperature, humidity, and with lighting that was controlled in a cycle of light 12 hours/dark 12 hours. All the rats underwent bilateral OVX, except for the normal group. The rats were then randomly divided into six groups ( $n=5$  for each group): normal, Sham (OVX + Sham), CPC with 2% ALE, 5% ALE, and 10% ALE groups. Three months after OVX, animals were anesthetized with intraperitoneal injections of 30 mg/kg pentobarbital sodium (Merck, Germany) before surgery. Under sterile conditions, a posterior midline incision was made along the proximal tail exposing the dorsal aspect of caudal vertebral bodies C4-C7. A 20-gauge needle was carefully inserted into the trabecular bone of the vertebral body via the distal endplates of C4-C7. By using a Kirschner wire, the defects were dilated along the longitudinal axis of the vertebrae. Vertebral body defects were filled with 0.1 ml of composite. The dorsal muscles and connective tissues were repositioned and closed in a routine manner. Prophylactic intramuscularly benzylpenicillin sodium was administered at the time of surgery and for three days postoperative. The study was approved by the Animal Care Committee of the Capital Medical University.

#### *Micro-CT analysis*

Micro-CT imaging (GE Health Care Co., USA) at  $16 \mu\text{m}$  isotropic voxel resolution was performed on the C5 of each group. Nomenclature and symbols were used to describe volumetric BMD, trabecular number (Tb.N), trabecular thickness (Tb.Th), and trabecular spacing (Tb.Sp). By using vertebral endplates as anatomical bony landmarks and a fixed region of interest (ROI), Tb.Th was determined from the average of direct measurements of the trabecular bone thickness of the caudal vertebral bodies. Similarly, analysis of the trabecular network (Tb.N and Tb.Sp) consisted of a  $1.0 \text{ mm}^3$  ROI used to sample trabecular bone at a specified site 1.0 mm from the vertebral endplate.<sup>30</sup>

#### *Biomechanical axial compression*

C6 were harvested from  $\text{CO}_2$  euthanized animals and individually loaded between two plate rods on an Instron machine. A compressive force was applied in the craniocaudal direction at a normal deformation rate of 0.1 mm/second. A load-displacement deformation curve was displayed with a monitoring recorder linked to the tester in each specimen. From the curve, failure force and stiffness of the vertebral bodies were obtained.

#### **Statistical analysis**

Data are expressed as mean  $\pm$  standard deviation (SD), and statistical analyses were performed using SPSS 13.0 (SPSS, Inc., Chicago, IL, USA). One-way analysis of variance (ANOVA) was conducted to assess differences among control, 2% ALE, 5% ALE, and 10% ALE groups. Mann-Whitney test was applied for multiple comparisons ( $n=5$ ). All statistical analysis was considered significant at a  $P < 0.05$ .

## RESULTS

### Structural properties of the specimens

The results from FTIR spectroscopy (Figure 1) were almost the same between the CPC and the CPC incorporating ALE. Only the ranges showing a small difference were presented for clarity. In the spectra of the cements, typical absorption bands could be found at  $1\ 060\ \text{cm}^{-1}$  because of stretching of the phosphate  $(\text{PO}_4)^{3-}$  groups. The peaks around  $1\ 420\ \text{cm}^{-1}$  and  $1\ 562\ \text{cm}^{-1}$  arose from hydroxyl (OH) bending and  $\text{CO}_3^{2-}$  vibrating. The typical absorption band from stretching of the OH groups in HA appears as a weak shoulder around  $3\ 334\ \text{cm}^{-1}$ .

### Morphology of the specimens

The cured products of CPC were observed by SEM, confirming their anisotropy and porosity (Figure 2). In addition, we found that the grain size and porosity of cured products of CPC and CPC containing different ALE concentrations were almost the same, although they showed a tendency to increase with the increase in ALE concentration.

### Setting time

The setting times of CPC, 2% ALE, 5% ALE, and 10% ALE were shown in Table 1. The initial and final setting times of the CPC were  $(10.10 \pm 0.74)$  and  $(23.70 \pm 1.20)$

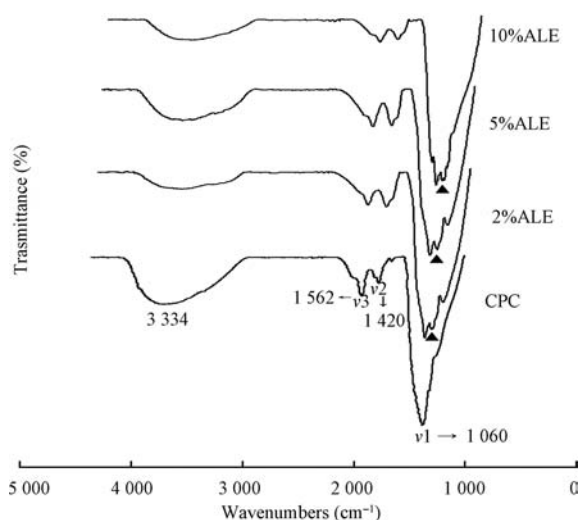


**Figure 1.** The FTIR of calcium phosphate cement (CPC), CPC + 2% alendronate (ALE), CPC + 5% ALE and CPC + 10% ALE ( $n=5$ ). Triangle indicated the very small difference between the CPC and composites.

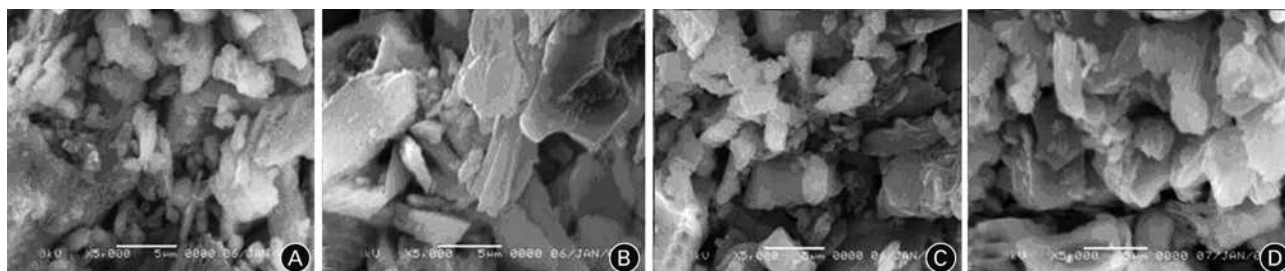


**Figure 2.** Scanning electron microscope (SEM) images of calcium phosphate cement (CPC) (A), 2% alendronate (ALE) (B), 5% ALE (C), and 10% ALE (D) samples (original magnification  $\times 5\ 000$ ).

minutes, respectively. ALE incorporated into the CPC prolonged the setting time of the composite. The higher the concentration of ALE, the longer the setting time was, and there were some significant differences between the groups ( $P < 0.05$ ).

### Compressive strength

There were variations in compressive strength between the CPC and the CPC containing different ALE concentrations. The strength of CPC was  $(13.000 \pm 0.595)$  MPa, of 2% ALE was  $(5.160 \pm 0.268)$  MPa, of 5% ALE was  $(5.540 \pm 0.233)$  MPa, and of 10% ALE was  $(5.360 \pm 0.552)$  MPa. The strength of the CPC was significantly higher compared with the other three groups ( $P < 0.01$ ). Although the strength of the 5% ALE group was higher than the 2% and 10% ALE groups, the difference was not significant ( $P > 0.05$ ).

### In vitro release

The *in vitro* cumulative release of ALE within 21 days from different specimens was illustrated in Figure 3. In release testing over the initial 5 days, a decline was found in the three groups, which had curves of similar shape, with a general exponential tendency, despite a burst of release at the beginning. Thus, there was a remarkably high release rate during the first 5 days. The concentrations of the released ALE then gradually slowed down during the subsequent 16 days. In 21 days, the released percentage of 2% ALE, 5% ALE and 10% ALE were 33.2%, 24.4%, and 20.8%, respectively. In addition, the early release rate of the high ALE content group was significantly greater than the low ALE content group ( $P < 0.01$ ).

### Cytotoxicity of specimens

Rat MSCs were incubated with eluant of CPC, CPC with 2% ALE, 5% ALE, and 10% ALE groups for 7 days to evaluate the cytotoxicity of the three ALE specimens.

**Table 1.** The setting times measured for the different groups ( $n=5$ , mean $\pm$ SD, minutes)

Groups	$T_i$	$T_f$
CPC (control)	$10.1 \pm 0.74$	$23.7 \pm 1.20$
2% ALE	$20.4 \pm 2.30^*$	$32.6 \pm 2.07^*$
5% ALE	$24.6 \pm 1.82^{*†}$	$39.2 \pm 3.19^{*†}$
10% ALE	$29.8 \pm 1.92^{*†}$	$47.8 \pm 2.39^{*†}$

$T_i$ : initial setting time;  $T_f$ : final setting time. \* $P < 0.01$ :  $T_i$  2% alendronate (ALE) compared with ALE 5%, and 2% ALE compared with 10% ALE;  $T_f$  2% ALE compared with ALE 5%, and 2% ALE compared with 10% ALE;  $†P < 0.05$ :  $T_i$  5% ALE compared with 10% ALE;  $T_f$  5% ALE compared with 10% ALE.

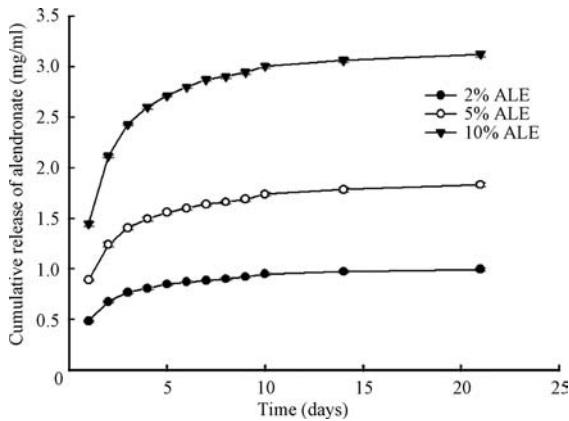


**Figure 3.** The cumulative release of ALE from CPC with different ALE concentrations. Error bars were shown as mean ± SD (n=5).

Figure 4 showed the results of the MTT tests, indicating that the number of viable cells in the culture medium increased with time of incubation. There were no significant differences between the groups. Within each group, there were significant differences at different times ( $P < 0.01$ ).

**Microstructural properties**

In the locally osteoporotic caudal vertebrae, the local treatment with ALE-loaded CPC significantly increased BMD ( $P < 0.05$ ) and Tb.N ( $P < 0.05$ ) compared with Sham group (Figure 5A and 5B), but BMD was not significantly different in treated groups compared with the CPC and normal groups. Moreover, there was no significant difference in Tb.N between the Sham and CPC group. Tb.SP was significantly higher in the Sham group than in the other groups (Figure 5C,  $P < 0.01$ ). However, there were no significant differences among the groups with regard to the Tb.Th (Figure 5D). The Sham group showed a marked deterioration in the microstructure of caudal vertebral trabeculae (Figure 6).

**Biomechanical properties**

Biomechanical strength was significantly increased in treated groups compared with the Sham group under axial compression testing of caudal vertebrae (Figure 7A,  $P < 0.05$ ). There were also similar changes in stiffness among groups (Figure 7B). In addition, stiffness was significantly

higher in the normal group than in the Sham and CPC groups, but there was no significant difference between the Sham and CPC groups. Furthermore, there were no significant differences among the normal, 2% ALE, 5% ALE, and 10% ALE groups with regard to strength and stiffness.

**DISCUSSION**

Local treatment of osteoporosis is a potential therapeutic strategy that involves the augmentation of osteoporotic bone with bioresorbable and bioactive cement mixed with ALE. Although several biomaterials have been used as vehicles for the transport and sustained release of anti-osteoporotic agents, there are some disadvantages including no degradation, low release rate, and insufficient support for the local osteoporotic bone.<sup>8,31</sup> However, CPC has been shown to be highly biocompatible in the *in vivo* setting as a bone void filler with the potential to be remodeled into normal bone.<sup>22,32</sup> Therefore, the purpose of the present study was to investigate CPC as a carrier material for releasing

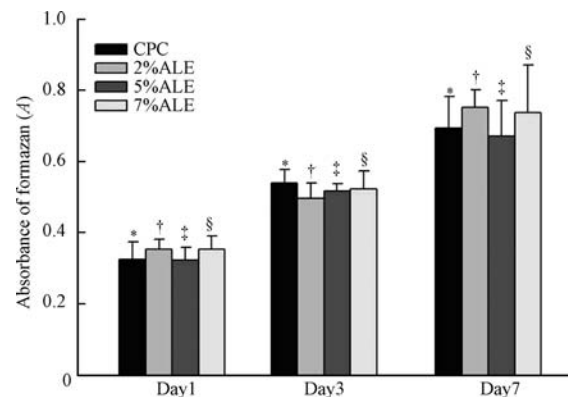


**Figure 4.** The MTT assay of rat mesenchymal stem cells (MSCs) cultured in 96-well plastic plates with eluant of CPC, 2% ALE, 5% ALE, and 10% ALE for 7 days (n=5). A: Absorbance. Subscripts 1, 3, and 7 represented at day 1, 3, and 7. \* $P < 0.01$ : CPC<sub>7</sub> compared with CPC<sub>3</sub> and CPC<sub>1</sub>, and CPC<sub>3</sub> compared with CPC<sub>1</sub>; † $P < 0.01$ : 2% ALE<sub>7</sub> compared with 2%; ALE<sub>1</sub> and 2% ALE<sub>3</sub>, and 2% ALE<sub>3</sub> compared with 2% ALE<sub>1</sub>; ‡ $P < 0.01$ : 5% ALE<sub>7</sub> compared with 5% ALE<sub>3</sub> and 5% ALE<sub>1</sub>, and 5% ALE<sub>3</sub> compared with 5% ALE<sub>1</sub>; § $P < 0.01$ : 10% ALE<sub>7</sub> compared with 10% ALE<sub>3</sub> and 10% ALE<sub>1</sub>, and 10% ALE<sub>3</sub> compared with 10% ALE<sub>1</sub>.

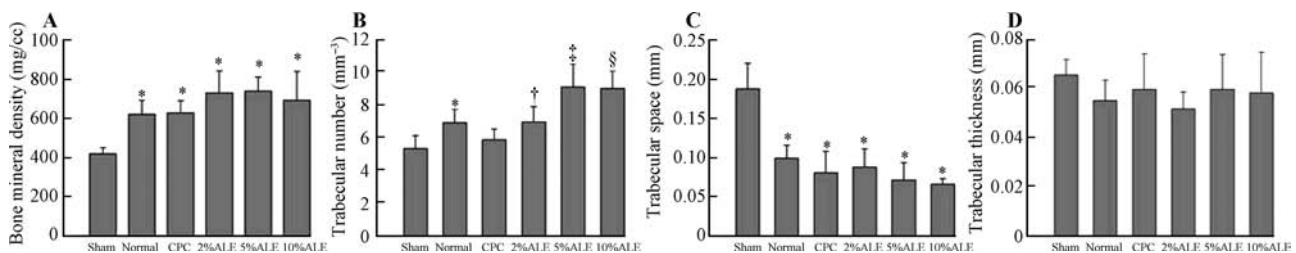


**Figure 5.** Microstructure in caudal vertebrae analyzed by micro-CT radiomorphometry (n=5). **A:** Sham group showed a significant decrease in BMD compared with other groups ( $P < 0.05$ ); but BMD was not significantly different between the treated groups and CPC or normal groups. **B:** There were significant increase in Tb.N in treated groups compared with CPC and Sham groups (normal group with CPC and Sham groups, \* $P < 0.05$ ; 2% ALE compared with CPC and Sham groups, † $P < 0.05$ ; 5% ALE compared with CPC and Sham groups, ‡ $P < 0.01$ ; 10% ALE compared with CPC and Sham groups, § $P < 0.01$ ). **C:** Tb.SP was significantly higher in the Sham group than in the other groups ( $P < 0.01$ ). **D:** There were no significant differences in Tb.Th among the groups.

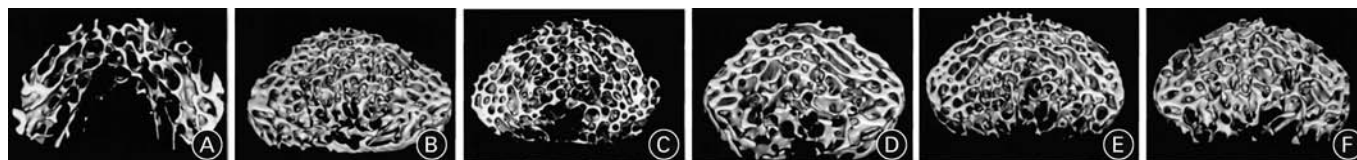


**Figure 6.** Effect of ovariectomized (OVX) and ALE-loaded CPC local treatment on 3D morphological changes in the rat osteoporotic caudal vertebrae. OVX induced a marked deterioration in microstructure of vertebral trabeculae (A), microstructure of vertebral trabeculae in normal (B), CPC alone (C), CPC with 2% ALE (D), 5% ALE (E), and 10% ALE (F).

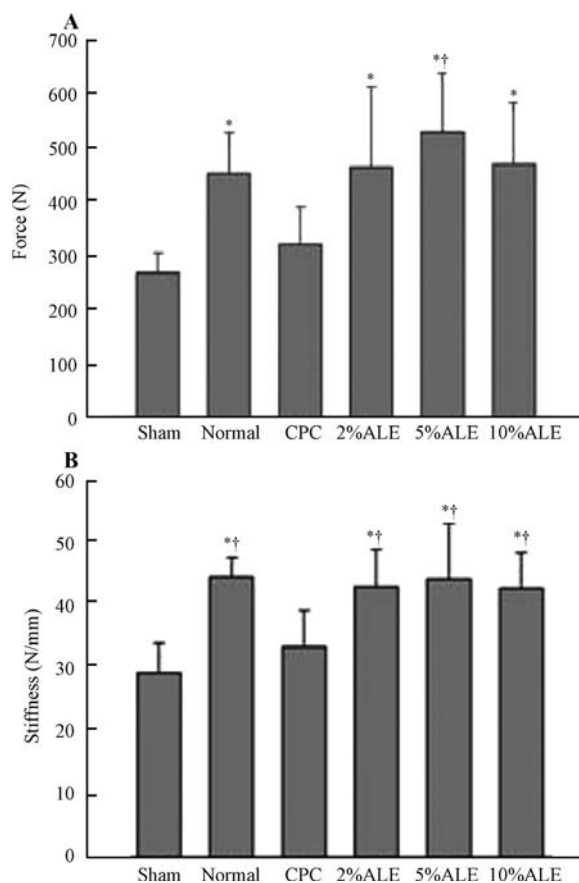


**Figure 7.** Axial compression testing of osteoporotic caudal vertebrae. Error bars represented standard deviation of five caudal vertebrae. **A:** Sham group exhibited significantly decreased strength compared with normal, 2% ALE, 5% ALE, and 10% ALE groups ( $^{\dagger}P < 0.05$ ), CPC group also exhibited significantly decreased strength compared with 5% ALE ( $^{\dagger}P < 0.05$ ). **B:** Sham group exhibited significantly decreased stiffness compared with normal, 2% ALE, 5% ALE, and 10% ALE groups ( $^{\dagger}P < 0.05$ ), CPC group also exhibited significantly decreased stiffness compared with the same groups ( $^{\dagger}P < 0.05$ )

ALE in local osteoporotic bone. To ensure that the ALE was left unchanged after mixing with the carrier material, the infrared spectrum, setting time, the microstructure, biomechanical strength, drug release, and cell cytotoxicity were analyzed *in vitro*.

The clusters of peaks in the FTIR profiles (Figure 1), around  $1\ 060\ \text{cm}^{-1}$ , demonstrated a typical apatite spectrum of  $\text{PO}_4^{3-}$ .<sup>33,34</sup> The  $3\ 334\ \text{cm}^{-1}$  bands were attributed to the OH stretching of DCPA and water.<sup>35</sup> These bands are characteristic of HA.<sup>36</sup> Small absorption bands in the spectra  $1\ 450\text{--}1\ 560\ \text{cm}^{-1}$  can be seen, indicating that  $\text{CO}_3^{2-}$ , at least partly, substitutes for  $\text{PO}_4^{3-}$  in the apatite lattice

(B-type  $\text{CO}_3^{2-}$ ).<sup>37</sup> The  $\text{CO}_3^{2-}$  is probably from atmospheric  $\text{CO}_2$ .<sup>38</sup> Small differences in the ranges might result from interference of foreign particles, which can be found in the spectrum of CPC. Hence, there is no obvious change to the characteristic CPC bands after ALE incorporation.

Setting time of the CPC can be affected or modified by introducing a drug either to the powder phase or its liquid phase, and as a consequence, the physicochemical and mechanical properties can change.<sup>39–42</sup> In generally, the setting time of CPC is normally 3–20 minutes.<sup>43</sup> In the current study, the values of the initial and final setting times of CPC were  $(10.1 \pm 0.74)$  and  $(23.7 \pm 1.20)$  minutes, respectively. The presence of ALE greatly affected both initial and final setting times, which increased with increasing concentrations of ALE, and there were significant differences among the groups. The lengthening of the setting times may be useful in applications requiring prolonged periods of composite handling and workability.<sup>44</sup> Furthermore, we noticed a marked reduction in mechanical strength when ALE was added into the CPC. The strength of the CPC was significantly higher compared with the three ALE groups ( $P < 0.01$ ). This decrease in mechanical strength was attributed to increased porosity and some inhibition of the setting reaction, as suggested by the presence of a certain amount of reactants when ALE was incorporated. Our findings were in accordance with Panzavolta et al<sup>44</sup> who documented similar decreases in setting time and mechanical strength. The mechanical strength of the composite roughly corresponded with the physiological compressive strength of human vertebral cancellous bone, which fell within a range of 2–20 MPa.<sup>45,46</sup> In theory, the composite should provide proper support within the vertebral body.

The results on ALE release suggested that the release rate from the composite increased with an increase in drug concentration in the cement, as reported in a previous paper.<sup>47</sup> The burst release was probably related to the surface-adsorbed drug particles dispersing rapidly from matrix into buffer in the first 5 days while the subsequent decline in release rate could be ascribed to the chelation between the cured product of CPC with HA and ALE. In addition, the higher release rate of the high drug content composite was probably a result of almost complete occupation of adsorption sites on the HA surface chelated with ALE molecules. There were more drugs in the physical adsorption state of supersaturation, which made the dissolution rate of ALE molecules from the surface of HA faster. In 21 days, the released percentage of 2%

ALE, 5% ALE, and 10% ALE were 33.2%, 24.4%, and 20.8%, respectively. Although it seemed a bit low relative to osteoporotic patients still exceeding the 70mg/60kg oral dose plasma concentrations of ALE,<sup>48,49</sup> and with the degradation of CPC, the released percentage could increase. In addition, Zhou et al<sup>50</sup> suggested that drug release involves two different mechanisms: drug molecule diffusion and polymer matrix degradation. We supposed this kind of delivery system involves the following two release processes: (1) the drug is first hybridized with CPC nanoparticles because of the high affinity of ALE for HA, and the release of ALE from the CPC is controlled by the solubility of the CPC, and (2) ALE is enclosed in the pores of the CPC, which induces a more significant retarded release of ALE from the composite matrix.

In addition, to evaluate the biocompatibility of ALE-loaded CPC materials, the P5 rats MSCs were incubated with eluant of CPC, 2% ALE, 5% ALE, and 10% ALE for 7 days, and the number of viable cells in the culture medium increased during this time. There were no differences between groups, whereas each group showed significantly higher values at 3 and 7 days compared to day 1. Also, the longer the duration, the larger the number of viable cells was. The specimens showed good biocompatibility in terms of the proliferation of the cells. The results were consistent with other reports concerning the cytotoxicity of ALE which was released from a bioactive matrix.<sup>37,51</sup>

The OVX rat caudal vertebrae as a model of postmenopausal spine bone loss has been well documented.<sup>30</sup> Oral ALE has already been widely used in the clinical treatment of osteoporosis.<sup>10,11,13</sup> To date, the local application of ALE on vertebral trabecular microstructure and biomechanical strength remains yet to be not fully elucidated. Here we showed that OVX rat caudal vertebral cancellous bone, treated by ALE-loaded CPC, exhibited a significant increase in BMD, Tb.N, strength, and stiffness and a decrease in Tb.SP compared with the Sham group.

The biomechanics of the caudal vertebrae is associated with numerous parameters, including bone mass, BMD, and the relative contributions of trabecular bone.<sup>52,53</sup> In the presence of diminished BMD, the altered trabecular bone has been implicated in the weakened biomechanical strength evident in the osteoporotic spine. Our findings revealed that estrogen deficiency significantly affected the bone microstructure of the caudal vertebrae in OVX rats. Six months after ovariectomy, there were significant changes in bone microstructure except for Tb.Th, similar to previous reports.<sup>54</sup> Among the total bone microstructure parameters, BMD were significantly higher in the treated groups and in the normal group compared with the Sham group ( $P<0.05$ ), but there were no significant differences between the CPC and the 2% ALE, 5% ALE, and 10% ALE groups. Tb.N was significantly higher in the 2% ALE, 5% ALE, 10% ALE, and normal groups compared with the sham and CPC groups; there were no significant differences between the 2% ALE, 5% ALE, and 10% ALE groups. In

addition, Tb.SP was significantly higher in the sham group than in the other groups. We found that the Tb.Th did not decrease during the progression of bone loss induced by OVX. Even the ALE-loaded CPC treated rats had thinner trabeculae, which may be due to compensatory responses that have been elucidated by other researchers.<sup>55,56</sup> However, the molecular mechanism of compensatory responses is unclear, and such a compensatory behavior did not overcome the biomechanical impairments caused by OVX.

In the *in vivo* study, we showed that the OVX rat caudal spine exhibited pathologic bone changes consistent with the osteoporosis phenotype. ALE-loaded CPC treating caudal vertebrae delayed the pathological changes of the trabecular bone microstructure induced by OVX. Of the *in vivo* study, CPC seemed to prevent osteoporosis as previously described.<sup>24</sup> However, it appeared hardly convincing with regard to Tb.N and biomechanical properties. This may be due to CPC not being fully absorbed, which led to some error on the parameters of BMD and Tp.SP. The 2% ALE, 5% ALE, and 10% ALE groups appeared to have therapeutic effects on the osteoporotic spine. Furthermore, 5% ALE demonstrated relatively better performance in compression strength compared with 2% ALE and 10% ALE, and exhibited significantly higher compression strength compared with CPC, while 2% ALE and 10% ALE did not. Despite the successful results, our study had several limitations. First, the OVX rat model could not completely represent the pathophysiologic condition of postmenopausal patients. In particular, it cannot represent the osteoporotic vertebral compression fracture. Second, the ROI of micro-CT may not be suitable for clinical examination. Because the group size was limited, the study was slightly underpowered to determine the statistical significance for all the assessed parameters, but we could see the trends. However, this does not affect our judgment about the effects of ALE-loaded CPC for local treatment of osteoporotic rat spine. Recently, some research suggested that the compressive strength of calcium sulfate cement (CSC) is better than CPC.<sup>57</sup> In addition, zoledronate (Reclast), the latest generation of an anti-osteoporotic drug that requires 5 mg once-a-year infusion, can treat postmenopausal osteoporosis. We have reasons to believe that CSC mixed with Reclast may have prospectives for treatment. It can not only overcome the slightly lower compressive strength of CPC, but also prolong the local anti-osteoporotic effect. Future advances should investigate the effects of the new composite in local osteoporotic bone and increase the sample size. Furthermore, we should inspect the BMD and bone microarchitecture at different time intervals and determine what happens when the bisphosphonate release stops.

In conclusion, CPC containing ALE as a DDS displayed satisfactory properties *in vitro*. The setting time increased with increased concentration of ALE. Although the addition of ALE decreased the mechanical strength of the composite, it still corresponded roughly to the physiological

compressive strength of human vertebral cancellous bone. In addition, a sustained release of ALE was observed over 21 days and the novel DDS had good biocompatibility. *In vivo*, the OVX rat caudal spine exhibited pathologic bone changes consistent with the osteoporosis phenotype. CPC seemed to prevent osteoporosis, but was hardly convincing with regard to its Tb.N and biomechanical properties. ALE-loaded CPC can enhance the OVX rat vertebral trabecular bone microarchitecture and biomechanical properties. Furthermore, 5% ALE demonstrated relatively better performance.

## REFERENCES

- Consensus development conference: prophylaxis and treatment of osteoporosis. *Am J Med* 1991; 90: 107-110.
- Li NH, Ou PZ, Zhu HM, Yang DZ, Zhao X, Zhang DX, et al. study on prevalence rate of fractures in the middle-aged and elderly population in parts of china (in Chinese). *Chin J Clin Rehabil* 2003; 7: 1284-1285.
- Roux S. New treatment targets in osteoporosis. *Joint Bone Spine* 2010; 77: 222-228.
- Greenspan SL, Beck TJ, Resnick NM, Bhattacharya R, Parker RA. Effect of hormone replacement, alendronate, or combination therapy on hip structural geometry: a 3-year, double-blind, placebo-controlled clinical trial. *J Bone Miner Res* 2005; 20: 1525-1532.
- Siris ES, Harris ST, Eastell R, Zanchetta JR, Goemaere S, Diez-Perez A, et al. Skeletal effects of raloxifene after 8 years: results from the continuing outcomes relevant to Evista (CORE) study. *J Bone Miner Res* 2005; 20: 1514-1524.
- Otsuka M, Oshinbe A, Legeros RZ, Tokudome Y, Ito A, Otsuka K, et al. Efficacy of the injectable calcium phosphate ceramics suspensions containing magnesium, zinc and fluoride on the bone mineral deficiency in ovariectomized rats. *J Pharm Sci* 2008; 97: 421-432.
- Peter B, Gauthier O, Laib S, Bujoli B, Guicheux J, Janvier P, et al. Local delivery of bisphosphonate from coated orthopedic implants increases implants mechanical stability in osteoporotic rats. *J Biomed Mater Res A* 2006; 76: 133-143.
- Phillips FM, Turner AS, Seim HB 3rd, MacLeay J, Toth CA, Pierce AR, et al. *In vivo* BMP-7 (OP-1) enhancement of osteoporotic vertebral bodies in an ovine model. *Spine J* 2006; 6: 500-506.
- Black DM, Cummings SR, Karpf DB, Cauley JA, Thompson DE, Nevitt MC, et al. Randomised trial of effect of alendronate on risk of fracture in women with existing vertebral fractures. *Lancet* 1996; 348: 1535-1541.
- Sharpe M, Noble S, Spencer CM. Alendronate: an update of its use in osteoporosis. *Drugs* 2001; 61: 999-1039.
- Bone HG, Hosking D, Devogelaer JP, Tucci JR, Emkey RD, Tonino RP, et al. Ten years' experience with alendronate for osteoporosis in postmenopausal women. *N Engl J Med* 2004; 350: 1189-1199.
- Black DM, Delmas PD, Eastell R, Reid IR, Boonen S, Cauley JA, et al. once-yearly zoledronic acid for treatment of postmenopausal osteoporosis. *N Engl J Med* 2007; 356: 1809-1822.
- Huang W, Wang YJ, Ren L, Du C, Shi XT. A novel PHBV/HA microsphere releasing system loaded with alendronate. *Mat Sci Eng C* 2009; 29: 2221-2225.
- Marshall JK, Thabane M, James C. Randomized active and placebo-controlled endoscopy study of a novel protected formulation of oral alendronate. *Dig Dis Sci* 2006; 51: 864-868.
- Strampel W, Emkey R, Civitelli R. Safety considerations with bisphosphonates for the treatment of osteoporosis. *Drug Safety* 2007; 30: 755-763.
- Poole KE, Compston JE. Osteoporosis and its management. *Br Med J* 2006; 333: 1251-1256.
- Migliorati CA. Bisphosphonates and oral cavity avascular bone necrosis. *J Clin Oncol* 2003; 21: 4253-4254.
- Delmas PD. Treatment of postmenopausal osteoporosis. *Lancet* 2002; 359: 2018-2026.
- Bohner M, Gbureck U, Barralet JE. Technological issues for the development of more efficient calcium phosphate cement: a critical assessment. *Biomaterials* 2005; 26: 6423-6429.
- Apelt K, Theisis F, El-Warrak AO, Zlinszky K, Bettschart-Wolfisberger R, Bohner M, et al. *In vivo* behavior of three different hydraulic calcium phosphate cements. *Biomaterials* 2004; 25: 1439-1451.
- Larsson S, Bauer TW. Use of injectable calcium phosphate cement for fracture fixation: a review. *Clin Orthop Relat Res* 2002; 395: 23-32.
- Ooms EM, Wolke JGC, Van de Heuvel MT, Jeschke B, Jansen JA. Histological evaluation of the bone response to calcium phosphate cement implanted in cortical bone. *Biomaterials* 2003; 24: 989-1000.
- Libicher M, Hillmeier J, Liegibel U, Sommer U, Pyerin W, Vetter M, et al. Osseous integration of calcium phosphate in osteoporotic vertebral fractures after kyphoplasty: initial results from a clinical and experimental pilot study. *Osteoporosis Int* 2006; 17: 1208-1215.
- Nosoudi N, Moztafzadeh F, Rabiee S, Gelinsky M, Nezafati N. Using bisphosphonate as a part of calcium phosphate cement in osteoporotic patients for local loosening prevention. *Bone* 2009; 44: S68-S98.
- Jindong Z, Hai T, Junchao G, Bo W, Li B, Qiang WB. Evaluation of a novel osteoporotic drug delivery system *in vitro*: alendronate-loaded calcium phosphate cement. *Orthopedics* 2010; 33: 561-570.
- ASTM Standard C191-03: Standard test method for time of setting of hydraulic cement by Vicat needle. ASTM International. 2002.
- Miao J, Liu CR, Wang JF, Wang Y, Hao LB, Mao KY, et al. Physicochemical properties of calcium phosphate cement incorporated with antibiotics. *Ortho J Chin* 2004; 12: 230-232.
- Kuljianin J, Jankovic' I, Nedeljkovic' J, Prstojevic' D, Marinkovic' V. Spectrophotometric determination of alendronate in pharmaceutical formulations via complex formation with Fe (III) ions. *J Pharm Biomed Anal* 2002; 28: 1215-1220.
- John R. W. Masters. Cytotoxicity and viability assays in animal cell culture: a practical approach, 3rd ed. Oxford University Press, Oxford 2000: 11-15.
- Wang ML, Massie J, Perry A, Garfin SR, Kim CW. A rat osteoporotic spine model for the evaluation of bioresorbable bone cements. *Spine* 2007; 7: 466-474.
- Long KA, Jackson JK, Yang C, Chehroudi B, Brunette DM, Burt HM. Controlled release of alendronate from polymeric films. *J*

- Biomater Sci Poly Ed 2009; 20: 653-672.
32. Kurashina K, Kurita H, Hirano M, Kotani A, Klein CP, de Groot K. *In vivo* study of calcium phosphate cements: implantation of an alpha-tricalcium phosphate/dicalcium phosphate dibasic/tetracalcium phosphate monoxide cement paste. *Biomaterials* 1997; 18: 539-543.
  33. Niedhart C, Maus U, Redmann E, Siebert CH. *In vivo* testing of a new *in situ* setting beta-tricalcium phosphate cement for osseous reconstruction. *J Biomed Mater Res* 2001; 55: 530-537.
  34. Liu DM, Yang Q, Troczynski T, Tseng WJ. Structural evolution of sol-gel-derived hydroxyapatite. *Biomaterials* 2002; 23: 1697-1687.
  35. Hofmann MP, Young AM, Gbureck U, Nazhat SN, Barralet JE. FTIR-monitoring of a fast setting brushite bone cement: effect of intermediate phases. *J Mater Chem* 2006; 16: 3199-3206.
  36. W.J. Lo, DM. Grant. Hydroxyapatite thin films deposited onto uncoated and (Ti, Al, V) N-coated Ti alloys. *J Biomed Mater Res* 1999; 46: 408-417.
  37. Van den Vreken N, Pieters IY, Declercq HA, Cornelissen MJ, Verbeeck RM. Characterization of calcium phosphate cements modified by addition of amorphous calcium phosphate. *Acta Biomater* 2010; 6: 617-625.
  38. Pieters IY, Maeyer EAPD, Verbeeck RMH. Stoichiometry of  $K^+$  and  $CO_3^{2-}$  containing apatites prepared by the hydrolysis of octacalcium phosphate. *Inorg Chem* 1996; 35: 5791-5797.
  39. Bohner M, Lemaitre J, Merckle HP, Gander B. Control of gentamicin release from a calcium phosphate admixed poly (acrylic acid). *J Pharm Sci* 2000; 89: 1262-1270.
  40. Takechi M, Miyamoto Y, Ishikawa K, Nagayama M, Kon M, Asaoka K, et al. Effects of added antibiotics on the basic properties of anti-washout-type fast-setting calcium phosphate cement. *J Biomed Mater Res* 1998; 39: 308-316.
  41. Ratier IR, Gibson SM, Best M, Freche M, Lacout JL, Rodriguez F. Behaviour of a calcium phosphate bone cement containing tetracycline hydrochloride or tetracycline complexed with calcium ions. *Biomaterials* 2001; 22: 897-901.
  42. Huang Y, Liu CS, Shao HF, Liu ZJ. Study on the applied properties of tobramycin-loaded calcium phosphate cement. *Key Eng Mater* 2000; 192: 853-860.
  43. Wang XP, Chen L, Xiang H, Ye J. Influence of anti-washout agents on the rheological properties and injectability of a calcium phosphate cement. *J Biomed Mater Res B Appl Biomater* 2006; 81: 410-418.
  44. Panzavolta S, Torricelli P, Bracci B, Fini M, Bigi A. Alendronate and Pamidronate calcium phosphate bone cements: Setting properties and *in vitro* response of osteoblast and osteoclast cells. *J Inorg Biochem* 2009; 103: 101-106.
  45. Keaveny TM, Hayes WC. A 20-year perspective on the mechanical properties of trabecular bone. *J Biomech Eng* 1993; 115: 534-542.
  46. McCalden RW, McGeough JA, Court-Brown CM. Age-related changes in the compressive strength of cancellous bone. *J Bone Joint Surg Am.* 1997; 79: 421-427.
  47. Otsuka M, Nakahigashi Y, Matsuda Y, Fox JL, Higuchi WI, Sugiyamac Y. A novel skeletal drug delivery system using self-setting calcium phosphate cement VIII: the relationship between *in vitro* and *in vivo* drug release from indomethacin-containing cement. *J Control Release* 1997; 43: 115-122.
  48. Yun MH, Kwon KI. High-performance liquid chromatography method for determining alendronate sodium in human plasma by detecting fluorescence: Application to a pharmacokinetics study in humans. *J Pharm Biomed Anal* 2006; 40: 168-172.
  49. Rhim SY, Park JH, Park YS, Lee MH, Kim DS, Shaw LM, et al. Bioavailability and bioequivalence of two oral formulations of alendronate sodium 70 mg: an open-label, randomized, two-period crossover comparison in healthy Korean adult male volunteers. *Clin Ther* 2009; 31: 1037-1045.
  50. Zhou SB, Deng XM, Li XB. Investigation on a Novel Core-Coated Microspheres Protein Delivery System. *J Control Release* 2001; 75: 27-36.
  51. Pignatello R, Cenni E, Micieli D, Fotia C, Salerno D, Avnet S, et al. A novel biomaterial for osteotropic drug nanocarriers: synthesis and biocompatibility evaluation of a PLGA-ALE conjugate. *Nanomedicine* 2009; 4: 161-175.
  52. Ma YL, Dai RC, Sheng ZF, Jin Y, Zhang YH, Fang LN, et al. Quantitative association between osteocyte density and biomechanics, microcrack and microstructure in OVX rats vertebral trabeculae. *J Biomech* 2008; 41: 1324-1332.
  53. Teo JCM, Si-Hoe KM, Keh JEL, Teoh SH. Correlation of cancellous bone microarchitectural parameter from microCT to CT number and bone mechanical properties. *Mater Sci Eng C* 2007; 27: 333-339.
  54. Boyd SK, Davision P, Muller R, Gasser JA. Monitoring individual morphological changes overtime in ovariectomized rats by *in vivo* micro-computed tomography. *Bone* 2006; 39: 854-862.
  55. Waarsing JH, Day JS, van der Linden JC, Ederveen AG, spanjers C, De Clerck N, et al. Detecting and tracking local changes in the tibiae of individual rats: a novel method to analyse longitudinal *in vivo* micro-CT data. *Bone* 2004; 34: 163-169.
  56. Sheng Z, Dai R, Wu X, Fang LN, Fan HJ, Liao EY. Regionally-specific compensation for bone loss in the tibial trabeculae of estrogen deficient rats. *Acta Radiologica* 2007; 48: 531-539.
  57. Zhang SD, Wang C, Jiang XJ, Yang HL, Tang TS. Experimental research on biomechanics of calcium sulfate cement in thoracolumbar burst fractures. *Ortho J Chin* 2009; 17: 1-5.

(Received July 15, 2014)

Edited by Chen Xin